



# Effects of different soil and water conservation measures on hydrological extremes and flood processes in the Yanhe River, Loess Plateau, China

ChaoJun Gu<sup>1,2</sup> · Yongqing Zhu<sup>1</sup> · Renhua Li<sup>1</sup> · He Yao<sup>1</sup> · Xingmin Mu<sup>2,3</sup>

Received: 9 January 2021 / Accepted: 4 June 2021 / Published online: 13 June 2021  
© The Author(s), under exclusive licence to Springer Nature B.V. 2021

## Abstract

The runoff and sediment load of the Loess Plateau have changed significantly due to the implementation of soil and water conservation measures since the 1970s. However, the effects of soil and water conservation measures on hydrological extremes have rarely been considered. In this study, we investigated the variations in hydrological extremes and flood processes during different periods in the Yanhe River Basin (a tributary of the Loess Plateau) based on the daily mean runoff and 117 flood event data from 1956 to 2013. The study periods were divided into reference period (1956–1969), engineering measures period (1970–1995), and biological control measures period (1996–2013) according to the change points of the annual streamflow and the actual human activity in the basin. The results of the hydrological high extremes ( $HF1_{\max}$ ,  $HF3_{\max}$ ,  $HF7_{\max}$ ) exhibit a decreasing trend ( $P < 0.01$ ), whereas the hydrological low extremes ( $HBF1_{\min}$ ,  $HBF3_{\min}$ ,  $HBF7_{\min}$ ) show an increasing trend during 1956–2013. Compared with the hydrological extremes during the reference period, the hydrological high extremes increased during the engineering measures period at low (<15%) and high frequency (>80%), whereas decreased during the biological control measures period at almost all frequencies. The hydrological low extremes generally increased during both the engineering measures and biological control measures periods, particularly during the latter period. At the flood event scale, most flood event indices in connection with the runoff and sediment during the engineering measures period were significantly higher than those during the biological control measures period. The above results indicate that the ability to withstand hydrological extremes for the biological control measures was greater than that for the engineering measures in the studied basin. This work reveals the effects of different soil and water conservation measures on hydrological extremes in a typical basin of the Loess Plateau and hence can provide a useful reference for regional soil erosion control and disaster prevention policy-making.

**Keywords** Hydrological extremes · Soil and water conservation · Flood events · Yanhe River Basin

✉ ChaoJun Gu  
chaojungu1990@163.com

Extended author information available on the last page of the article

## 1 Introduction

The flow regime of streams and rivers worldwide has suffered from drastic changes due to global warming and anthropogenic intervention in recent decades (Milly 2005; Wang et al. 2016a, b). Global warming leads to higher evaporation rates and enables the atmosphere to transport higher amounts of water vapor, resulting in the acceleration of the hydrological cycle (Menzel and Burger, 2002). Thus, the occurrence and intensification of extreme hydrological events worldwide will increase (Easterling et al. 2000; Herschy 2002; Milly, 2002). According to statistics, major rivers in China have experienced floods since the 1990s (e.g., Yangtze River floods in 1991 and 1998; Yellow River floods in 1977, 1981, 2013, and 2017; Pearl River floods in 1994 and 1996; Haihe River flood in 1996; Minjiang River flood in 1998; Hanjiang River floods in 2003 and 2005; and Huaihe River floods in 2003, 2005, and 2007), causing huge losses of the gross domestic product (Zhiyong et al. 2012). Furthermore, human activities affect hydrological regimes mainly by altering surface conditions and soil properties in a variety of ways, such as land-use changes, irrigation, logging activity, mining, soil and water conservation measures, and reservoir construction (Jorge et al. 1998; Yang et al. 2019).

Numerous studies have focused on the changes in hydrological regimes in different rivers at various spatiotemporal scales (Milly 2005; Wang et al. 2015; Villarini et al. 2012; Wang et al. 2016a, b; Wan et al. 2020). At a global scale, Milly et al. (2005) found that streamflow exhibited an increasing trend in Central North America and northern Australia, and decreased in southern Australia, southern Europe, South America, and sub-Saharan Africa largely because of the impacts of human activities. At the national scale, Burn and Elnur et al. (2002) analyzed the trend characteristics of the streamflow of 248 catchments in Canada during the 1950s–2000s and revealed that the reason for the changes in the streamflow climatic conditions varied. At the basin scale, Jorge et al. (1998) investigated trends in the hydrological parameters of the Piracicaba River Basin located in the southeastern region of Brazil using statistical tests. Their results indicated that total precipitation and evapotranspiration showed significant increasing trends for the entire basin; however, half of the streamflow gauge stations demonstrated significantly decreasing trends due to large-scale human consumption. In terms of hydrological extremes, Villarini et al. (2012) analyzed extreme flooding in Austria over the period 1951–2006 from 27 stations and found that seven of these showed a significant decreasing trend because of human activities, four stations showed a significant increasing trend, and the remaining changed insignificantly. In China, many researchers have explored the hydrological regimes at the basin scale, particularly for the two largest Chinese rivers (i.e., Yangtze River and Yellow River) (Piao et al. 2010; Wang et al. 2013; Gu et al. 2019a; Bao et al. 2019). Moreover, the results of Wang et al. (2013) showed that annual runoff for the entire Yellow River exhibited a significant downward trend during 1950–2008, whereas a significant decreasing trend for Yangtze River was found only in its upper reaches over the same period. Zhang et al. (2011) investigated the hydrological extremes in the Poyang Lake Basin and found that the 7-day high flow changed insignificantly after the construction of water reservoirs, except the Wan'an water reservoir, owing to the limitation of the design standards of the water reservoirs.

The Loess Plateau is one of the most severely eroded areas globally and is an important agricultural area in China. Soil erosion leads to the loss of soil nutrients and the destruction of soil structures (e.g., porosity and aggregates), which has a negative effect on the growth of vegetation and causes a vicious cycle of the regional ecological environment (Gao et al.

2017; Bao et al. 2019). To control soil erosion, numerous soil conservation measures have been implemented since the 1950s. In 1999, the government sponsored the “Grain for Green” program, which was implemented to mitigate improper and excessive land use with the aim of reducing sediment transport and increasing water supply. The implementation of large-scale water and soil conservation measures significantly changed the underlying surface conditions (e.g., vegetation coverage, microtopography, and soil property) in the Loess Plateau, further influencing the hydrological regimes in the area. Compared with the period 1960–1979, the sediment transport and runoff reduced by approximately 90% and 50%, respectively, during 2000–2015 (Gu et al. 2019a). Numerous studies considered that dam construction, terrace projects, water diversion and irrigation, and ecological management were the main factors for runoff and sediment reduction, and most scholars believe that ecological construction activities, particularly vegetation restoration, were the main reasons (Gao et al. 2017; Liu et al. 2017).

The Yanhe River Basin is a tributary of the Yellow River, located almost in the center of the Loess Plateau, and is a typical hilly-gully area. This basin has experienced much eco-friendly construction since the 1970s, leading to significant changes in the hydrological regimes. Gao et al. (2015) examined the trends and shifts in the streamflow regime from 1953 to 2010 and found that annual streamflow decreased significantly with a change point in 1996, but no significant trend and change point in base flow was found. They further discovered that biological measures (e.g., revegetation, planting trees, and grass) and engineering measures (e.g., fish-scale pits, horizontal trenches, and sediment-trapping dams) play an important role in the reduction of streamflow. Zhao et al. (2014a, b) evaluated the influence of vegetation restoration on runoff and sediment load of the Yanhe River Basin and found that the soil and water conservation dominated by vegetation restoration contributed 17.5% and 55.9% toward the runoff and sediment load decline, respectively. Although the hydrological processes and effects of human activities in the Yanhe River Basin have been greatly studied, little attention has been given to the hydrological extremes in the region. Compared with normal hydrological regimes, the impacts of extreme hydrological changes on environments and social economy are much greater. The global flood cost has been revealed to reach a total of \$470 billion since 1980 (HSBC, 2011). Approximately 196 million people in more than 90 countries were found to be exposed on average every year to catastrophic flooding (UNDP, 2004). In the Yanhe River Basin, two massive floods occurred since the 1950s, that is, July 1977 and July 2013. In July 1977 (mainly on days 5 and 6), the flood inundated the Yan’an City (the central city of the Yanhe River Basin) and submerged many houses, licking up many people’s lives (Fan et al. 1989). The flood in July 2013 lasted for approximately a month. Continuous heavy rainfall caused a large number of cave houses to collapse, landslides, mudslides, road congestion, farmland damage, and more, which affected a total of 1.545 million people’s estates and caused a direct economic loss of \$1.46 billion (Huang et al. 2014; Zhou et al. 2015). However, the runoff and sediment in the river course were much lower than those in July 1977 (Gu et al. 2017). The disasters, flood characteristics, and sediment transport caused by these two floods in the Yanhe River Basin were largely different due to the significant change of the underlying surface in the basin. Accordingly, strengthening the available research regarding changes in extreme hydrological events and their affecting factors has a very important practical significance (Martinez and Le Toan, 2007) and has caused widespread concern (Nie et al. 2012).

This study aimed to (1) examine trends and probability behaviors in hydrological extremes during different periods in the Yanhe River, (2) investigate flood characteristics during different periods, and (3) explore the possible causes behind changes in hydrological

extremes. Such information can help managers evaluate the effects of different soil and water conservation measures on hydrological extremes in the past half century, thereby guiding future resource utilization and disaster prevention in this region.

## 2 Data and methods

### 2.1 Study area

The Yan River is a first-order branch of the Yellow River, China. It originates from the Zhou Mountain in Jingbian County and flows approximately 300 km through Zhidan and Ansai counties, Baota District, and Yanchang County of Yan'an City, and eventually into the Yellow River in Yanchang County. The Yan River Basin ( $36^{\circ}21'–37^{\circ}19'N$ ,  $108^{\circ}38'–110^{\circ}29'E$ ) is located in the middle of the Loess Plateau, covering an area of  $7,687 \text{ km}^2$  (Fig. 1). The Ganguyi hydrological station is the downstream control station of the basin with a drainage area of  $5852 \text{ km}^2$ . The climate region of the Yan River Basin is north temperate continental monsoonal, in which the average annual precipitation and air temperature are approximately 500 mm and  $9^{\circ}\text{C}$ , respectively. Soil erosion is severe throughout the basin due to unsustainable land-use management, low vegetation cover, erodible soils, and frequent high-intensity summer storms, which cause enormous sedimentation and high flood risks downstream, including the Yellow River (Gao et al. 2015). To reduce soil erosion, large-scale soil and water conservation measures have been implemented since the 1970s (Table 1). The periods of soil and water conservation in the basin can be divided into two stages (Zhao et al. 2014a, b): the first from 1970 to 1995, in which many terraces and check dams were built in the basin (Table 1). Although the area of afforestation and grass planting also increased during this period, the proportion of the total area of the basin was small. After 1996, the area of afforestation and grass planting increased significantly due to the launch of the “Grain for Green” program in 1999. Compared with 1996, the areas of afforestation, grass planting, and

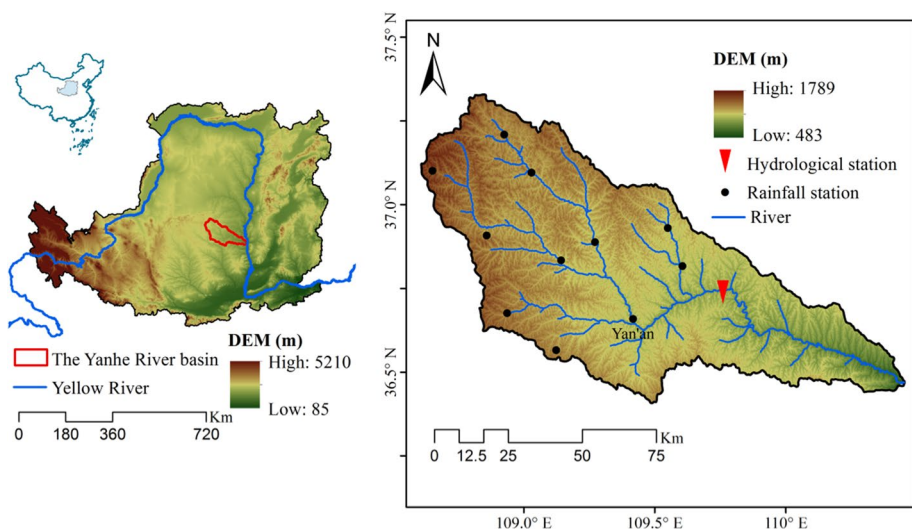


**Fig. 1** Location of the Yanhe River basin and hydrological and rainfall stations within the basin

**Table 1** Changes of cumulative area of each soil and water conservation measures in the Yanhe River Basin

Year	Terrace (km <sup>2</sup> )	Check dam (km <sup>2</sup> )	Afforestation (km <sup>2</sup> )	Grass planting (km <sup>2</sup> )	Blockading administration (km <sup>2</sup> )
1959	4.33	7.41	64.94	0.57	0.00
1969	49.45	25.40	253.39	6.46	0.00
1979	102.18	46.10	450.82	30.24	0.00
1989	182.63	60.65	1320.95	251.34	18.00
1996	288.73	66.86	1668.32	449.84	35.63
2009	344.46	72.53	1887.15	495.44	99.06
2013	350.87	73.29	1920.28	484.51	111.97

blockading administration increased by 15.1%, 7.7%, and 214.2% in 2013, respectively. However, the area of terraces and check dams increased inconspicuously after 1996 (Table 1).

## 2.2 Data

The daily mean runoff data at Ganguyi hydrological gauging station from 1956 to 2013 were used to calculate the hydrological extremes. In this study, the 1-day high flow ( $HF1_{\max}$ ), 3-day high flow ( $HF3_{\max}$ ), and 7-day high flow ( $HF7_{\max}$ ) are defined as the hydrological high extremes. The 1-day minimum base flow ( $HBF1_{\min}$ ), 3-day minimum base flow ( $HBF3_{\min}$ ), and 7-day minimum base flow ( $HBF7_{\min}$ ) are defined as the hydrological low extremes. Additionally, the data of rainfall (obtained from seven rainfall stations within the basin, Fig. 1), runoff, and suspended sediment concentration (SSC) of flood events during 1977–2013 (data during 1990–2006 were missing) at Ganguyi station were collected to investigate the changes in flood characteristics during different periods in the basin. The above data were obtained from the Hydrological Year Book of the Yellow River issued by the Yellow River Conservancy Commission (YRCC) of the Ministry of Water Resources of the People's Republic of China (PRC). The land-use data (1990, 2005) were provided by the Data-Sharing Network of China Earth System Science ([www.geodata.cn](http://www.geodata.cn)). ArcGIS 10.1 was used to process the land-use data. All measured data used in this study were checked by the corresponding agencies and rated as good quality.

## 2.3 Methodologies

### 2.3.1 Base flow separation

Base flow was calculated from daily mean values of streamflow using the two-parameter digital filter separation method proposed by Eckhardt, 2005. This method can estimate stable base flow and is the optimal base flow separation method for use in the Loess Plateau (Lei et al. 2011). The method calculates base flow as follows:

$$q_{bi} = \frac{\alpha(1 - B_{\max})q_{b(i-1)} + (1 - \alpha)B_{\max}q_i}{1 - \alpha B_{\max}} \quad (1)$$

where  $q_{bi}$  is the base flow on day  $i$ ;  $q_i$  is the streamflow at day  $i$ ;  $\alpha$  is the filtering factor, which is appropriate for many regions when it is 0.925 (Nathan and McMahon, 1990; Arnold and Allen, 1999); and  $B_{\max}$  is the greatest base flow factor. Eckhardt recommends  $B_{\max}$  values of 0.80 for a regular stream dominated by pore aquifers, 0.50 for a seasonal stream dominated by pore aquifers, and 0.25 for a regular stream dominated by a weak pervious layer. In this study,  $B_{\max}=0.45$  was obtained by optimization (Gao et al. 2015).

### 2.3.2 Cumulative anomaly method

The cumulative anomaly method is widely used in the analysis of change points in hydro-meteorological elements (Wang et al. 2015). The anomaly accumulation at year  $t$  ( $\hat{X}_t$ ) can be estimated using:

$$\hat{X}_t = \sum_{i=1}^t (x_i - \bar{x}) \quad t = 1, 2, \dots, n \quad (2)$$

where

$$\bar{x} = \frac{1}{n} \sum_{t=1}^n x_t \quad (3)$$

in which  $x_t$  is the value of the hydrometeorological element at year  $t$ ,  $n$  is the data series length of the hydrometeorological element.

The continuous increase in  $\hat{X}_t$  indicates that the element anomaly in this time interval is continuously positive, i.e., to say, the element in this period are persistently more than the  $n$ -year average of the element; inversely, the element in this period is lower than the  $n$ -year average if  $\hat{X}_t$  continuous decrease. The inflection point of the curves of the cumulative anomaly can be deemed as the possible change points of the element. To determine the actual change points, the  $t$ -test method can be used. When the absolute value of the  $t$ -test statistics (IU) of the possible change points is higher than 1.64 (1.96), then the change points are valid at the 0.05 (0.01) significance level.

### 2.3.3 Statistical tests for trend analysis

The nonparametric Mann–Kendall (MK) trend test is widely used to detect the changing trends in hydroclimatic variables because it is robust for non-normally distributed and censored data (Mann 1945). The test identifies trends according to the calculation of a standardized statistic ( $Z$ ). A positive  $Z$  value indicates an upward trend, and vice versa.  $|Z| \geq 1.96$  (2.56) suggests that the trend is significant at the 0.05 (0.01) significance level. Detailed description of this method is provided in Mann (1945) and Kendall (1975). Afterward, if a linear trend is present, a simple nonparametric procedure developed by Sen (1968) can estimate the change magnitude per unit time, as follows:

$$\beta = \text{Median} \left( \frac{x_j - x_i}{j - i} \right) \text{ where } \forall i < j \quad 1 < i < j < n \quad (4)$$

where  $\beta$  is the median over all combinations of record pairs for the whole data denoting the slope of the trend, and  $n$  is the data length.

### 2.3.4 Frequency analysis

The *Pearson type III* frequency distribution has been extensively used in China (Wu et al. 2013) and is recommended for calculating the design flood. Therefore, this frequency distribution was applied to analyze the frequency characteristics of the Yanhe River during different periods. The distribution pattern of the *Pearson type III* was calculated as follows:

$$f(x) = \frac{(\beta)^\alpha}{\Gamma(\alpha)}(x - a_0)^{\alpha-1} e^{-\beta(x-a_0)} \tag{5}$$

where  $\Gamma(\alpha)$  is the gamma function of  $\alpha$ ;  $\alpha$ ,  $\beta$ , and  $a_0$  are the shape, size, and location parameters of the *Pearson type III* function. The parameters were estimated as follows:

$$\alpha = \frac{4}{C_S^2} \tag{6}$$

$$\beta = \frac{2}{\bar{x}C_v C_S} \tag{7}$$

$$a_0 = \bar{x} \left( 1 - \frac{2C_v}{C_S} \right) \tag{8}$$

where  $\bar{x}$  is the average value of the time series sample,  $C_v$  is the coefficient of variation of the time series sample, and  $C_s$  is the coefficient of skew of the time series sample. The above parameters were calculated as follows:

$$C_S = \frac{1}{n} \sum_{i=1}^n (x_i - \bar{x})^3 / \left[ \frac{1}{n} \sum_{i=1}^n (x_i - \bar{x})^2 \right]^{3/2} \tag{9}$$

$$\bar{x} = \frac{1}{n} \sum_{i=1}^n x_i \tag{10}$$

$$C_v = s/\bar{x} \tag{11}$$

$$s = \sqrt{\frac{1}{n} \sum_{i=1}^n (x_i - \bar{x})^2} \tag{12}$$

where  $s$  is the mean square error of the time series sample,  $x_i$  is the time series sample, and  $n$  is the data length.

### 2.3.5 Flood event indices

For each flood event, six runoff and sediment indices were used to describe the individual flood hydrographs and sediment load characteristics. The indices were the flood duration  $T$  (min), maximum runoff discharge  $Q_{max}$  (m<sup>3</sup>/s), maximum suspended sediment

concentration  $SSC_{max}$  ( $\text{kg}/\text{m}^3$ ), mean suspended sediment concentration  $SSC_{mean}$  ( $\text{kg}/\text{m}^3$ ), flood runoff depth  $H$  (mm), and sediment yield  $SY$  ( $\text{t}/\text{km}^2$ ).  $SSC_{mean}$ ,  $H$ , and  $SY$  were calculated using the following equations:

$$SY(t_1, t_2) = \frac{\int_{t_1}^{t_2} SSC_t Q_t dt}{A} = \frac{\sum SSC_t Q_t \Delta t}{A} \quad (13)$$

$$H(t_1, t_2) = \frac{\int_{t_1}^{t_2} Q_t dt}{A} = \frac{\sum Q_t \Delta t}{A} \quad (14)$$

$$SSC_{mean} = \frac{\sum SSC_t Q_t \Delta t}{\sum Q_t \Delta t} \quad (15)$$

where  $\Delta t$ ,  $Q_t$ , and  $SSC_t$  are the observed time interval, instantaneous flow discharge, and SSC for a specific flood event, respectively;  $A$  is the controlled area of the Ganguyi hydrologic station.

### 3 Results

#### 3.1 Temporal variations in annual streamflow and base flow

The accumulative anomaly curve of annual streamflow increased first, then stabilized after 1970, and decreased after 1996 (Fig. 2a). The results of the  $t$ -test indicate that the change points of 1970 and 1996 were significant at the 0.05 and 0.01 significance levels, respectively. Hence, the annual streamflow change from 1956 to 2013 was divided into three periods: 1956–1969, 1970–1995, and 1996–2013. According to the implementation time of the soil and water conservation in the basin (Table 1), the period of 1956–1969 is considered as the reference period (P1), whereas those of 1970–1995 and 1996–2013 are considered as the engineering measures period (P2) and biological control measures period (P3), respectively.

Annual streamflow showed a significant decreasing trend during 1956–2013, with the reduction rate of  $15.5 \text{ m}^3/(\text{s}\cdot\text{a})$  ( $P < 0.01$ ) (Fig. 2b). Moreover, the mean annual streamflow exhibited distinct differences across the three periods. During P1, the mean annual streamflow was  $2,910.4 \text{ m}^3/\text{s}$ , which is 25.3% higher than that of the whole period ( $2,322.1 \text{ m}^3/\text{s}$ ). Meanwhile, the average annual streamflow values during P2 and P3 were 2,312.9 and  $1,877.8 \text{ m}^3/\text{s}$ , which are 20.5% and 35.5% less than that during P1, respectively. The annual base flow showed an insignificant temporal trend over the study period ( $P > 0.05$ ) (Fig. 2c), whereas the base flow index showed a significant increasing trend with an increasing rate of 0.003 per year ( $P < 0.01$ ) (Fig. 2d). The base flow index was 0.23 during P1, 0.31 during P2, and 0.358 during P3, which are 24.7% lower, 1.5% higher, and 17.1% lower than the mean value of the whole period (0.306).

Intra-annual changes in streamflow and base flow also displayed clear differences in the three periods (Fig. 3). Streamflow showed unimodal distribution throughout the year, among which more than 50% of the streamflow occurred during June–September (days 177–270). The streamflow generally declined during P2 and P3 compared with P1, particularly during June–September. However, the intra-annual change in streamflow



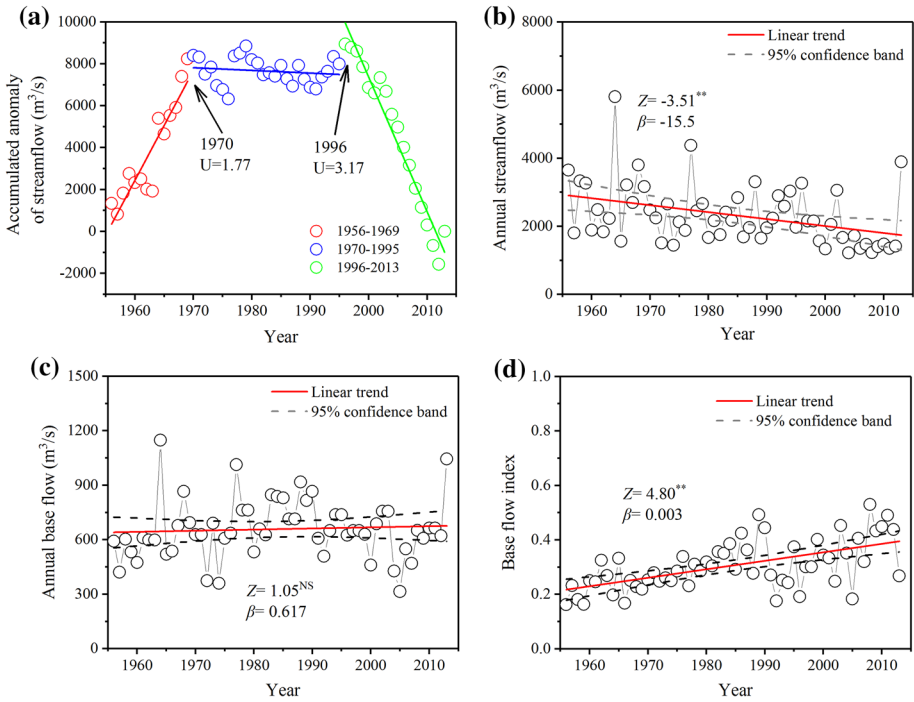


**Fig. 2** Accumulative anomaly curve of annual streamflow **a**, and interannual change of annual streamflow **b**, base flow **c**, and base flow index **d** in the Yanhe River

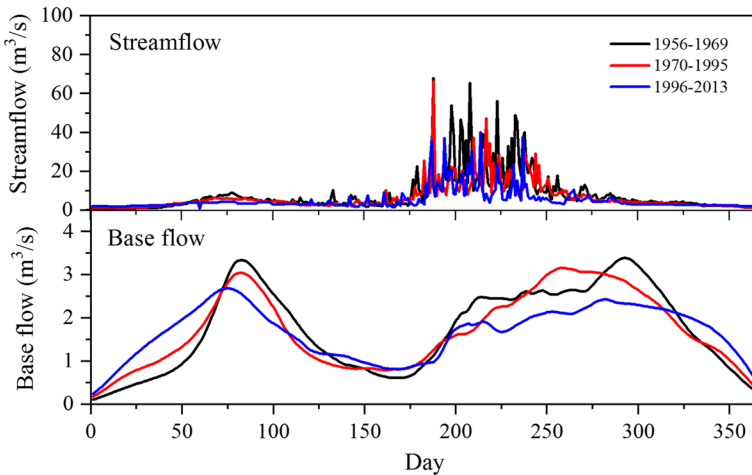


**Fig. 3** Daily streamflow and base flow during different periods within the year

became more even during P2 and P3 relative to P1. The proportions of streamflow during June–September account for 63.1%, 59.4%, and 53.6% of the annual streamflow during P1, P2, and P3, respectively. Furthermore, the intra-annual change in base flow exhibited

a bimodal pattern, with more than 20% of the flow appearing during March–April (days 61–120) and more than 50% occurring between mid-July and November (days 194–330). The base flow generally decreased during March–April and July–November during P2 and P3, but increased in the other months.

### 3.2 Temporal variations in hydrological extremes

The mean values of annual  $HF1_{max}$ ,  $HF3_{max}$ , and  $HF7_{max}$  between 1956 and 2013 were 252.54, 357.8, and 470.36  $m^3/s$ , respectively. The maximum and minimum of the high hydrological extreme indices occurred in 1977 and 2008, respectively. The mean values of annual  $HBF1_{min}$ ,  $HBF3_{min}$ , and  $HBF7_{min}$  were 0.16, 0.54, and 1.52  $m^3/s$ , respectively. The hydrological high extreme indices decreased significantly during 1956–2013, with the reduction rate ranging from 2.35 to 3.71  $m^3/(s \cdot a)$ . However, the hydrological low extremes indices increased significantly over the study period, among which the rate of increase varied from 0.002 to 0.016  $m^3/(s \cdot a)$ .

The hydrological high extreme indices generally increased during P1 and P2 and significantly decreased during P3 (Fig. 4a–c). The  $HF1_{max}$ ,  $HF3_{max}$ , and  $HF7_{max}$  decreased

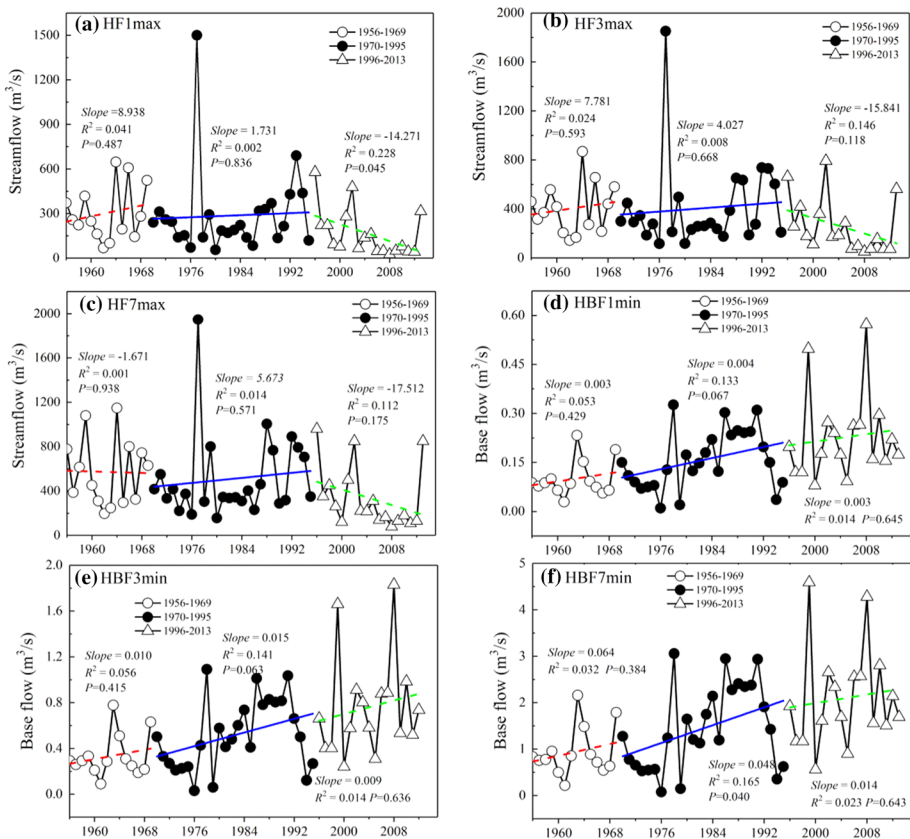


**Fig. 4** Change of hydrological extremes indices in the Yanhe River (The lines were the linear trend for each periods)

by 5.8%, 28.3%, and 29.2%, respectively, during P3 compared with their long-term average (1956–2013). The reduction rates of  $HF1_{max}$ ,  $HF3_{max}$ , and  $HF7_{max}$  during P3 were 14.3, 15.8, and 17.5  $m^3/(s \cdot a)$ , respectively. However, the hydrological low extreme indices increased during the three periods (Fig. 4d–f), particularly during P3. Compared with the mean values of 1956–2013,  $HBF1_{min}$ ,  $HBF3_{min}$ , and  $HBF7_{min}$  increased by 43.5%, 41.2%, and 39.9% during P3, respectively (Table 2).

### 3.3 Frequency characteristics of hydrological extremes during different periods

The parameters of the *Pearson type III* curves of the six hydrological extremes during different periods are shown in Table 3, and the probability and cumulative distribution functions of the hydrological extreme indices are shown in Fig. 5. The goodness of the *Pearson type III* curve ranged from 0.890 to 0.981, indicating that the *Pearson type III* distribution could significantly represent the probability behaviors of the hydrological extremes.

The frequency characteristics of hydrological extremes varied distinctly during the three periods (Figs. 6 and 7). Regarding the hydrological high extremes,  $HF1_{max}$ ,  $HF3_{max}$ , and  $HF7_{max}$  during P2 increased compared with those during P1 at frequencies < 15% and frequencies > 80% (Fig. 7a). However, the magnitude of the hydrological high extremes at almost all frequencies decreased during P3 compared with the hydrological high extremes during P1 (Fig. 7b). Considering the hydrological low extremes,  $HBF1_{min}$ ,  $HBF3_{min}$ , and  $HBF7_{min}$  increased during P2 and P3 at any frequency compared with those during P1, except for the frequency > 90% during P2 (Fig. 7). Moreover, the magnitude of the hydrological low extremes during P3 at the same frequency was higher than that of the low hydrological extremes during P2 (Fig. 7).

The three hydrological high extremes of any return periods significantly increased during P2 compared with P1 (Fig. 8a–c). However, the magnitudes of  $HF1_{max}$  and  $HF7_{max}$  decreased during P3 relative to P1 (Fig. 8a and c). Moreover,  $HF3_{max}$  of the <40 return period decreased, whereas that of the >40 return period increased (Fig. 8b). The magnitudes of  $HBF1_{min}$ ,  $HBF3_{min}$ , and  $HBF7_{min}$  showed increasing trends during P3 and P2 compared with those during P1 (Fig. 8d–f). Moreover, the increasing magnitudes of the hydrological low extremes during P3 were higher than those during P2. Table 4 displays the return periods of various magnitudes of the hydrological extreme indices. It shows that the return periods of the hydrological high extreme indices during P1 and P3 were larger than those of P2. However, the return periods of most hydrological low extreme indices during P2 and P3 were smaller than those during P1, particularly for P3.

**Table 2** Statistical parameters of the hydrological extreme indices in the Yanhe River during 1956–2013

Items	HF1max	HF3max	HF7max	HBF1min	HBF3min	HBF7min
Mean ( $m^3/s$ )	252.54	357.80	470.36	0.16	0.54	1.52
Maximum ( $m^3/s$ )	1500.00 (1977)	1851.30 (1977)	1946.70 (1977)	0.57 (2008)	1.83 (2008)	4.59 (1999)
Minimum ( $m^3/s$ )	24.90 (2008)	51.90 (2008)	79.10 (2008)	0.01 (1976)	0.03 (1976)	0.07 (1976)
MK trend	-2.88**	-2.57**	-2.73**	4.04**	3.86**	2.93**
$\beta$ value ( $m^3/(s \cdot a)$ )	-2.35	-2.79	-3.71	0.002	0.008	0.016

\*\*Significantly changed at  $P \leq 0.05$

**Table 3** The parameters of the hydrological extreme indices in the Yanhe River during different periods

Items	1956–1969			1970–1995			1996–2013					
	Mean (m <sup>3</sup> /s)	C <sub>V</sub>	C <sub>S</sub>	R <sup>2</sup>	Mean (m <sup>3</sup> /s)	C <sub>V</sub>	C <sub>S</sub>	R <sup>2</sup>	Mean (m <sup>3</sup> /s)	C <sub>V</sub>	C <sub>S</sub>	R <sup>2</sup>
	HF1max	303.68	0.72	1.23	0.977	286.08	1.55	5.27	0.899	269.98	1.25	2.52
HF3max	405.06	0.61	1.13	0.981	404.17	1.15	3.88	0.890	254.07	1.09	2.24	0.975
HF7max	572.1	0.63	1.08	0.969	509.71	0.94	3.31	0.927	334.39	1.03	2.26	0.939
HBFImin	0.09	0.78	1.22	0.916	0.15	0.72	0.14	0.977	0.22	0.76	1.58	0.941
HBFI3min	0.31	0.77	1.33	0.930	0.50	0.73	0.19	0.976	0.72	0.73	1.45	0.937
HBFI7min	0.88	0.77	1.22	0.941	1.42	0.75	0.27	0.967	2.01	0.65	0.84	0.958

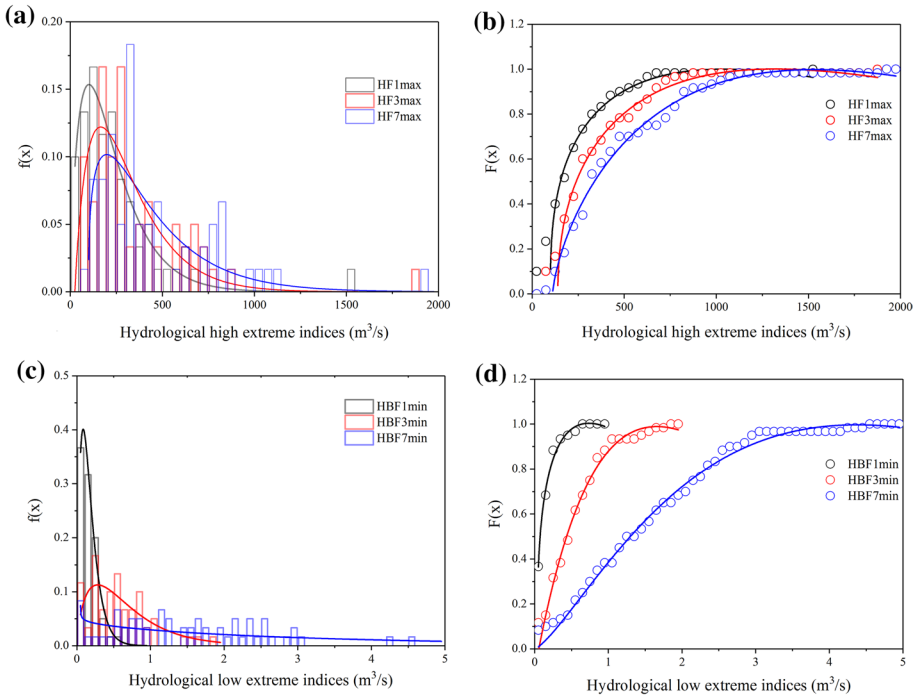


**Fig. 5** Probability and cumulative distribution functions of the hydrological extreme indices at the Ganguyi station (The lines were the fitting line for each indices)

### 3.4 Flood characteristics during different periods

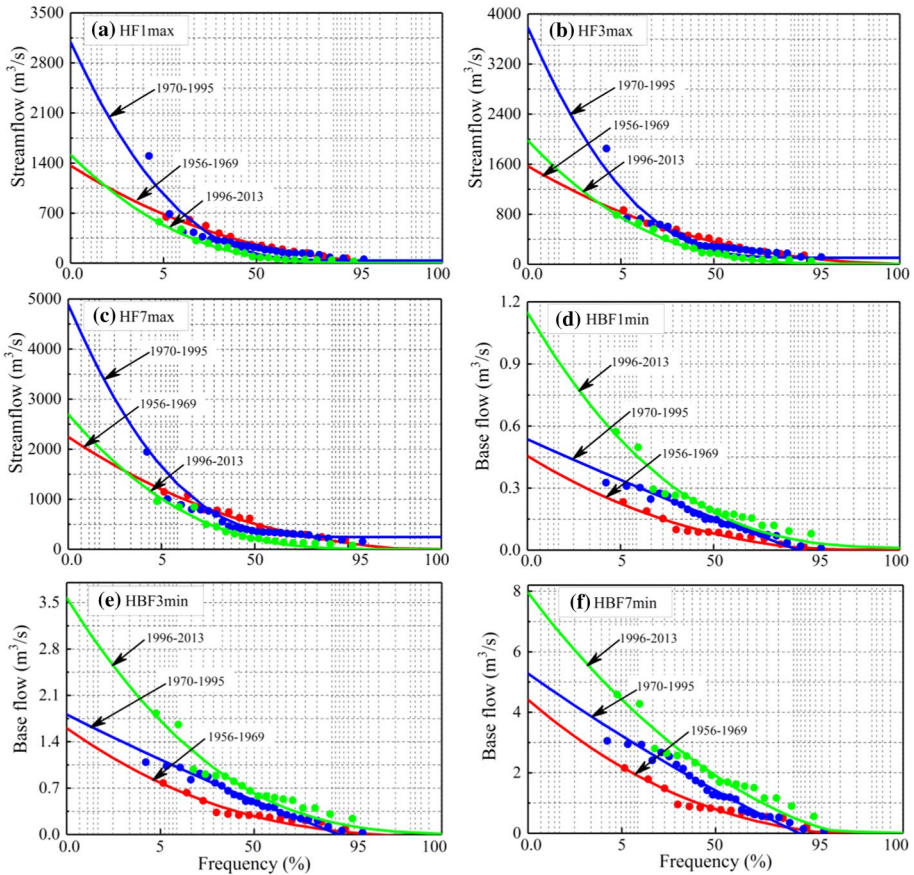
The characteristics of the flood events showed significant differences during the different periods (Fig. 9).  $Q_{max}$ ,  $SSC_{max}$ ,  $SSC_{mean}$ ,  $H$ , and  $SY$  in 2006–2013 were significantly lower than those during 1977–1989 ( $P < 0.01$ ). For instance,  $H$  and  $SY$  were 6.2 mm and 2,262.1 t/km<sup>2</sup> in the former period, which decreased to 3.3 mm and 315.1 t/km<sup>2</sup> in the latter period, respectively.

Figure 10 displays two typical flood processes in the Yanhe River: the flood event recorded on July 5, 1977, and that on July 25, 2013 (Fig. 10a and b, respectively). The two flood events lasted up to approximately 35 h and comprised multi-flood peak discharge and sediment peak values. Compared with the flood on July 25, 2013, the flow discharge and SSC was much larger for that on July 5, 1977, although the precipitation was similar.

## 4 Discussions

### 4.1 Driving forces of hydrological regime changes

Climate change and anthropogenic interventions have been widely recognized as significant driving forces of hydrological regime changes. The temperature in the Yanhe



**Fig. 6** Frequency characteristics of hydrological extremes during different periods (The lines were the fitting line for each indices)

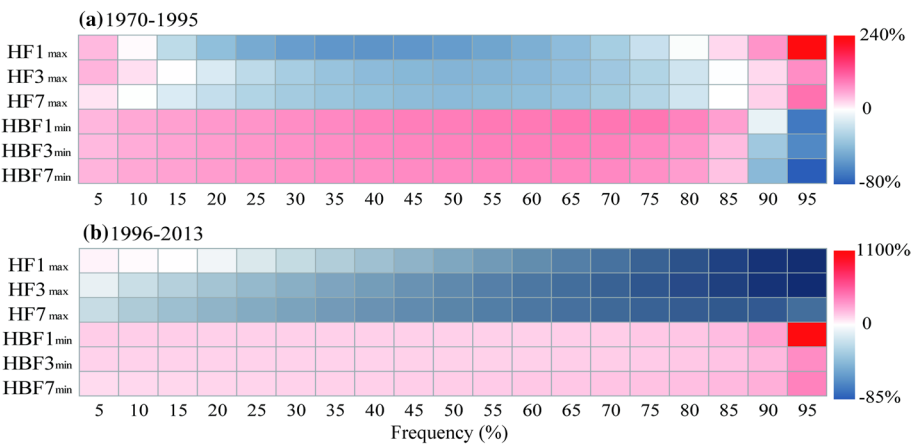


**Fig. 7** Change rate of the hydrological extreme indices during 1970–1995 **a** and 1996–2013 **b** relative to the period 1956–1969

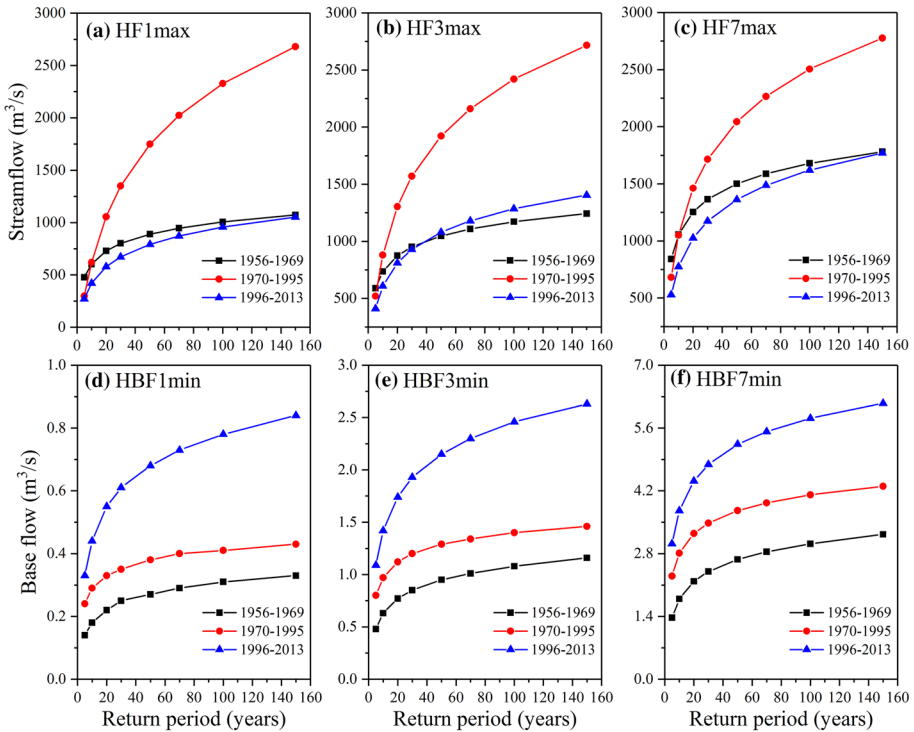


**Fig. 8** Comparisons of return periods of the hydrological extremes during different periods

**Table 4** Return periods of the hydrological extreme indices under various magnitudes during different periods

Items	Flow (m <sup>3</sup> /s)	Occurrence time	Return periods of 1960–1969 (year)	Return periods of 1970–1995 (year)	Return periods of 1996–2013 (year)
HF1max	1500.0	1977	> 500	37	> 500
HF3max	1851.3	1977	> 500	45	> 500
HF7max	1946.7	1977	291	291	239
HBF1min	0.57	2008	8	2	2
HBF3min	1.83	2008	> 500	> 500	24
HBF7min	4.28	2008	> 500	144	17

River Basin has increased significantly in the last 50 years with the progression of global warming (Gao et al. 2015). Warmer temperatures would increase evaporation and intensify drought, which would reduce streamflow. Furthermore, rainfall would become more nonuniform as the hydrological cycle is accelerated due to temperature increase, leading to an increase in extreme rainfall (Sun et al. 2016). Extreme rainfall increases the streamflow and sediment in a river basin, which has been demonstrated as the main driving force of hydrological regimes and sediment changes in loess areas

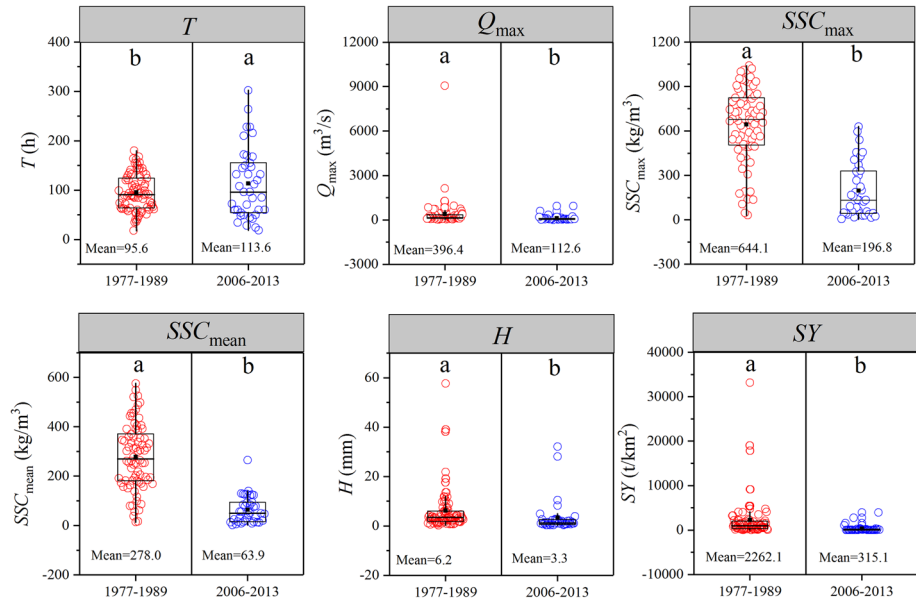


**Fig. 9** Characteristics of the flood events in different periods (Note: The different letters at the top of each sub-figure indicate the differences are significant at  $P < 0.01$  level;  $T$ , event flood duration;  $Q_{max}$ , event peak discharge;  $SSC_{max}$ , event maximum suspended sediment concentration;  $SSC_{mean}$ , event average suspended sediment concentration;  $H$ , event flood runoff depth;  $SY$ , event sediment yield)

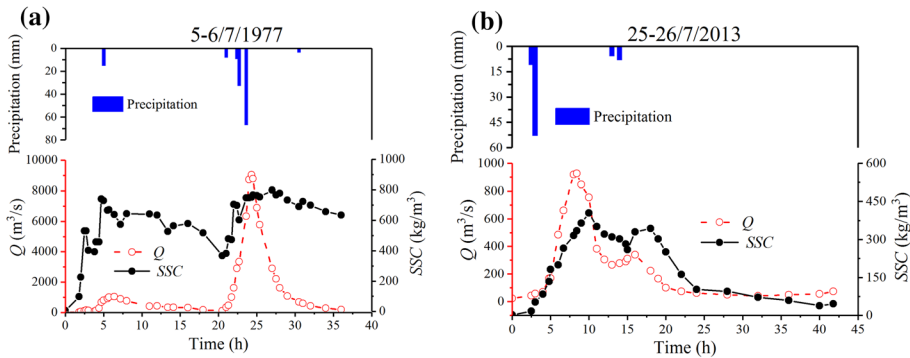


**Fig. 10** Two typical flood processes in the Yanhe river

(Angulo-Martínez and Beguería, 2009). Therefore, it is of great significance to study hydrological extremes at the basin scale.

As in many other basins in the Loess Plateau, the main anthropogenic interventions in the Yanhe River Basin are the soil and water conservation activities (Kang et al. 2001; Wang et al. 2016a, b). Abundant terraces and check dams were built in the Yanhe River Basin during the 1970–1980s for rapid control of soil erosion (Gao et al. 2015). After the 1980s, the implementation of soil and water conservation practices was significantly accelerated. With the support of the “Grain for Green” program, the total area of afforestation,



grass planting, and blockading administration grew rapidly after 1999 (Table 1). However, the areas of terraces, check dams, and grassland increased slightly because of the strict policy of returning farmland. Undoubtedly, the rapid adoption of soil and water conservation measures has played an important role in streamflow reduction in the Yanhe River Basin. Engineering measures, such as terrace, fish-scale pits, horizontal trenches, and sediment-trapping dams, have intercepted more hill slope runoff and small channel runoff into the mainstream river (Xu et al. 2004; Yuan and Lei, 2004). Furthermore, biological measures (e.g., revegetation, planting trees, and grass) reduce the conversion of rainfall to runoff by intercepting rainfall, increasing soil water storage, and vegetation evaporation/transpiration (Kang et al. 2001; Brown et al. 2013).

Land use/cover has clearly been transformed in the Yanhe River Basin with the implementation of soil and water conservation measures, which would have a significant impact on hydrological regimes (Bao et al. 2019). There was a net increase of 788.9 km<sup>2</sup> (20.3%) in grassland areas and 117.9 km<sup>2</sup> (8.2%) in forestland areas in 2010 relative to 1990 (Fig. 11). In contrast, the area of arable land decreased by 940.7 km<sup>2</sup> (50% of the total area, 1990). The land-use/cover change data show an increase in forested and grassland areas and a decrease in arable land, resulting in a significant increase in the vegetation coverage of the basin. The vegetation coverage increased to 52.3% in 2013, which is 64.9% higher than that of the vegetation coverage in the 1980s (31.7%) (Fig. 11c). The better growth of the vegetation could trap and absorb more water by

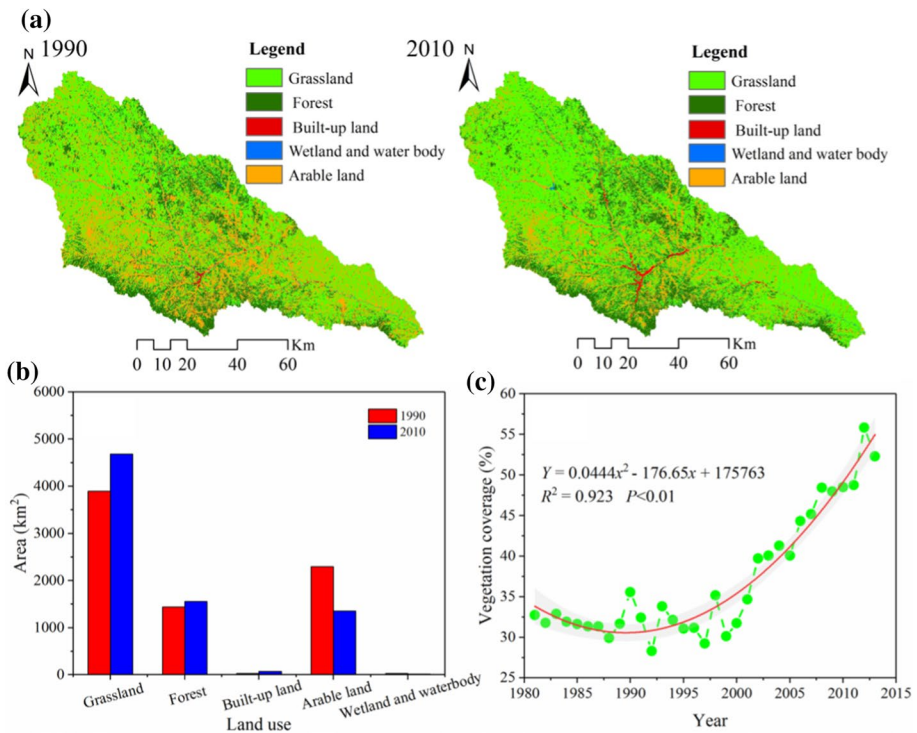


**Fig. 11** Land-use/cover change of the Yanhe River basin in 1990 and 2010 (a), the change of land use between 1990 and 2010 (b), and the vegetation coverage change during 1981–2013 (c)

the plants and eventually consumed by evapotranspiration, further resulting the surface runoff and SSL (Zhao et al. 2014a, b). According to previous studies, the contribution rates of human activities and climate change to the reduction in annual streamflow were almost equal in the Yanhe River Basin (Gao et al. 2015).

#### 4.2 Effects of different soil and water conservation measures on hydrological extremes

The changes in hydrological regimes and their driving factors in the Loess Plateau have been extensively studied (Gao et al. 2017; Liang et al. 2015; Gu et al. 2019a). However, hydrological extreme changes due to soil and water conservation measures have rarely been researched. In this study, we found that hydrological high extremes decreased significantly whereas the hydrological low extremes increased significantly over the past half century, indicating that soil and water conservation measures also significantly impact hydrological extremes (Table 2). The changing direction of the hydrological high extremes was consistent with the annual runoff and sediment in the River, while changing direction of the hydrological low extremes was inverse (Zhao et al. 2014a, b). Moreover, the changing trends of the hydrological extremes were different during the three periods, suggesting that the effects of different soil and water conservation measures on hydrological extremes were distinct (Fig. 4). The hydrological high extremes, i.e.,  $HF1_{\max}$ ,  $HF3_{\max}$ , and  $HF7_{\max}$ , during 1970–1995 increased significantly at high and low frequencies and generally increased during 1996–2013 compared with the hydrological high extremes during 1956–1969 at the same frequency and return period (Figs. 7 and 8). These results indicate that engineering measures could not effectively reduce the hydrological high extremes. Moreover, engineering measures (e.g., check dams and terraces) are susceptible to damage by severe rainstorms, which also restrict the functions of engineering measures in terms of controlling hydrological extremes. As Liang (2015) addressed, the number of reserved check dams peaked in the 1970s and decreased since the 1980s, as many of them gradually lost their function because of intensive rainfall, frequent floods, or requiring maintenance. When a dam is destroyed, there would be a substantial increase in runoff and sediment in the corresponding river, such as the flood on July 5, 1977. Zhang et al. (2011) investigated the hydrological extremes in the Poyang Lake basin (a river basin in southern China), and also found that the 7-day high flow ( $HF7$ ) were increasing after the construction of water reservoirs due to the limitation of the reservoirs storage capacity.

The hydrological low extreme indices, i.e.,  $HBF1_{\min}$ ,  $HBF3_{\min}$ , and  $HBF7_{\min}$ , increased significantly during 1970–1995 and 1996–2013 compared with the hydrological low extremes during 1956–1969 at the same frequency and return period (Fig. 7). Moreover, the increasing magnitudes of the hydrological low extremes during 1996–2013 were much higher than those of 1970–1995, indicating that biological measures could greatly increase the base flow in a river basin. Compared with the engineering measures, extensive vegetation construction in hillslopes increases rainfall intercept, soil infiltration capacity, and runoff resistance, which is long lasting for extreme hydrological protection (Gu et al. 2019b). Moreover, an increase in the soil infiltration capacity directly increases soil water, which would release the base stream during the dry season (Gu et al. 2019b). This is the main reason for the streamflow becoming more uniform during 1996–2013 (Fig. 3) and the base flow index significant increases.

### 4.3 Hydrological and sediment dynamics at the event scale

The Loess Plateau is the most severely eroded area in China owing to its low vegetation cover, frequent heavy storms, and large hilly plateau areas (Wang et al. 2016a, b; Gu et al. 2019a). The soil losses of the region caused by individual heavy storms can account for 60%–90% of the annual soil losses, which reflects the significance of investigating the hydrological extremes in this area (Fang et al. 2008). Since the 1970s, the large-scale implementation of soil and water conservation measures has significantly changed the underlying conditions, thereby causing changes in the hydrological regimes. In this study, we compared the flood characteristics during 1977–1989 with those during 2006–2013. The results show that the event flood duration ( $T$ ) during 2006–2013 was significantly higher than that during 1977–1989, whereas other flood event indices during 2006–2013 were significantly lower than those of 1977–1989 (Fig. 9). The result was in accordance with the study on the Xichuan River basin, a tributary of the Yanhe Rive (Hu et al. 2019). These indicate that soil and water conservation measures could also play an important role in sediment reduction under the condition of heavy rainstorms, particularly for vegetation restraint measures. The relationship between  $SY$  and  $H$  demonstrates that the correlation coefficient of  $SY$ – $H$  was higher during 1977–1989 than during 2006–2013 (Fig. 12a). Moreover, the slope of the linear function of 1977–1989 was much higher than that of 2006–2013, suggesting that the  $SY$  capacity of the basin during 2006–2013 was lower than that during 1977–1989. Additionally, vegetation restoration reduces the soil bulk density and increases soil porosity and soil aggregate stability, which is beneficial for increasing soil infiltration and reducing streamflow (Gu et al. 2019b). Meanwhile, the vegetation root system enhances soil erosion and corrosion resistance, which protects the soil from the loss of highly erodible finer particles. Considering the floods on July 5–6, 1977 and July 25–26, 2013, as examples, soil particles were clearly attenuated (Fig. 12b). These results illustrate that the function of the long-term vegetation restoration to sediment reduction was superior to the engineering measures.

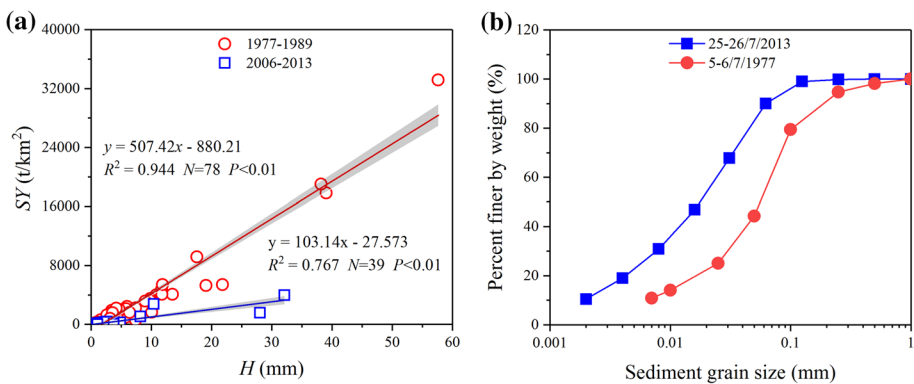


**Fig. 12** The relationship between sediment yield and runoff depth during different periods at flood events **a** and the particle size distribution curve of the soil during flood event in 5–6 July 1977 and 25–26 July 2013 **b**

## 5 Conclusions

The hydrological extremes and the 117 flood events during the different periods from 1956 to 2013 were investigated in the Yanhe River Basin. The annual streamflow showed a significant decreasing trend at the rate of  $15.5 \text{ m}^3/(\text{s}\cdot\text{a})$  and two change points in 1970 and 1996. Over the same period, the hydrological high extremes ( $\text{HF1}_{\text{max}}$ ,  $\text{HF3}_{\text{max}}$ ,  $\text{HF7}_{\text{max}}$ ) decreased significantly whereas the hydrological low extremes ( $\text{HBF1}_{\text{min}}$ ,  $\text{HBF3}_{\text{min}}$ ,  $\text{HBF7}_{\text{min}}$ ) increased significantly.

The effects of biological control measures in decreasing hydrological high extremes and increasing hydrological low extremes were found to be higher than the engineering measures. Compared with the hydrological extremes at the same frequency and return period during the reference period (1956–1969), the hydrological high extremes increased at the low ( $< 15\%$ ) and high ( $> 80\%$ ) frequencies during the engineering measures (e.g., check dam and terrace) period (1970–1995), whereas almost all decreased during the biological control measures (e.g., vegetation restoration and afforestation) period (1996–2013). However, the hydrological low extremes increased during both the engineering measures period and the biological control measures period. Moreover, the increasing amplitude during the biological control measures period was much higher than that during the engineering measures period. The results indicate that the biological control measures could effectively alleviate hydrological drought and flooding, whereas the functions of the engineering measures in terms of flood control were limited due to their vulnerability to flooding.

At the flood event scale, the maximum runoff discharge ( $Q_{\text{max}}$ ), maximum suspended sediment concentration ( $\text{SSC}_{\text{max}}$ ), mean suspended sediment concentration ( $\text{SSC}_{\text{mean}}$ ), flood runoff depth ( $H$ ), and sediment yield ( $SY$ ) during the engineering measures period were significantly higher than those during the biological control measures period ( $P < 0.05$ ), further indicating that the function of the biological control measures in reducing the runoff and sediment yield in flood events was greater than that of the engineering measures.

**Acknowledgements** This work was supported by National Natural Science Foundation of China (4207072131) and (41671285), the National Key Research and Development Program of China (2016YFC0501707, 2016YFC0402401).

**Author's contribution** Chaojun Gu carried out data processing, data analysis and wrote the paper. Yongqing Zhu designed the research framework. Renhua Li, He Yao, and Xingmin Mu offered guidance to complete the work and made revisions to the manuscript.

### Declarations

**Conflict of interest** The authors declare that there is no conflict of interest.

## References

- Angulo-Martínez M, Beguería S (2009) Estimating rainfall erosivity from daily precipitation records: a comparison among methods using data from the ebro basin (ne spain). *J Hydrol* 379(1):111–121
- Arnold JG, Allen PM (1999) Automated Methods for Estimating Baseflow and Ground Water Recharge From Streamflow Records. *J Am Water Resour Assoc* 35(2):411–424
- Bao Z, Zhang J, Wang G, Chen Q, Wang J (2019) The impact of climate variability and land use/cover change on the water balance in the middle yellow river basin, china. *J Hydrol* 577:123942

- Brown AE, Western AW, McMahon TA, Zhang L (2013) Impact of forest cover changes on annual streamflow and flow duration curves. *J Hydrol* 483:39–50
- Burn DH, Elnur MA (2002) Detection of hydrologic trends and variability. *J Hydrol* 255(1):107–122
- HSBC, (2011) Climate investment update. HSBC Global Research. [www.research.hsbc.com](http://www.research.hsbc.com). Accessed 13 Oct
- Easterling DR (2000) Climate extremes: observations, modeling, and impacts. *Science* 289(5487):2068–2074
- Eckhardt K (2005) How to construct recursive digital filters for baseflow separation. *Hydrol Proc* 19(2):507
- Fan RS, Yan FC (1989) Rainstorm flood in July 1977. *J China Hydrol* 1:52–57 (In Chinese)
- Fang HY, Cai QG, Chen H, Li QY (2008) Temporal changes in suspended sediment transport in a gullied loess basin: the lower Chabagou Creek on the Loess Plateau in China. *Earth Surf Proc Landform* 33:1977–1992
- Gao P, Jiang G, Wei Y, Mu X, Wang F, Zhao G, Sun W (2015) Streamflow regimes of the Yanhe River under climate and land use change, Loess Plateau China. *Hydrol Process* 29(10):2402–2413
- Gao P, Deng J, Chai X, Mu X, Zhao G, Shao H (2017) Dynamic sediment discharge in the hekou-longmen region of yellow river and soil and water conservation implications. *Sci Total Environ* 578(1):56–66
- Gu CJ, Mu XM, Sun WY, Gao P, Zhao GJ (2017) Comparative analysis of the responses of rainstorm flood and sediment yield to vegetation rehabilitation in the Yanhe River Basin. *J Nat Resour* 32(10):1755–1767 (In Chinese)
- Gu C, Mu X, Gao P, Zhao G, Sun W (2019a) Changes in run-off and sediment load in the three parts of the Yellow River basin, in response to climate change and human activities. *Hydrol Process* 33(4):585–601
- Gu CJ, Mu XM, Gao P, Zhao GJ, Sun WY, John T (2019b) Influence of vegetation restoration on soil physical properties in the loess plateau, china. *J Soils Sediments* 19:716–728
- Herschey RW (2002) The world's maximum observed floods. *Flow Measure Instrument*. [https://doi.org/10.1016/S0955-5986\(02\)00054-7](https://doi.org/10.1016/S0955-5986(02)00054-7)
- Hu J, Zhao G, Mu X, Tian P, Gao P, Sun W (2019) Quantifying the impacts of human activities on runoff and sediment load changes in a loess plateau catchment, china. *J Soils Sediments* 19(11):3866–3880
- Huang YH, Feng W, Li ZG (2014) Characteristics and geological disaster mode of the rainstorm happened on July 3, 2013 in Yanan Area of Shaanxi Province. *J Catastrophol* 29(2):54–59
- Kang SZ, Zhang L, Song XY, Zhang SH, Liu XZ, Liang YL, Zheng SQ (2001) Rainfall and land runoff and sediment loss responses use in two agriculture catchments on the Loess Plateau of China. *Hydrol Process* 15:977–988
- Kendall MG (1975) Rank correlation methods. Griffin, London, UK
- Lei YN, Zhang XP, Zhang JJ, Liu EJ, Zhang QY, Chen N (2011) Suitability analysis of automatic baseflow separation methods in typical watersheds of water-wind erosion crisscross region on the Loess Plateau, China. *Sci Soil Water Conserv* 9(6):57–64 (in Chinese)
- Li X, Zhang Q, Xu CY, Ye X (2015) The changing patterns of floods in poyang lake, china: characteristics and explanations. *Nat Hazards* 76:651–666
- Liang W, Bai D, Wang F, Fu B, Yan J, Wang S (2015) Quantifying the impacts of climate change and ecological restoration on streamflow changes based on a budyko hydrological model in china's loess plateau. *Water Resour Res* 51(8):6500
- Liu XY, Ma SY, Dang SZ (2017) Processes of sediment yield in the Yellow River basin in recent hundred years. *J Sed Res* 42(05):1–6
- Mann HB (1945) Non-Parametric Test against Trend. *Econometrika* 13:245–259
- Martinez JM, Toan T (2007) Mapping of flood dynamics and spatial distribution of vegetation in the Amazon floodplain using multitemporal SAR data. *Remote Sens Environ* 108(3):209–222
- Menzel L, Bürger G (2002) Climate change scenarios and runoff response in the mulde catchment (southern elbe, germany). *J Hydrol* 267(1):53–64
- Milly PCD, Wetherald RT, Dunne KA, Delworth TL (2002) Increasing risk of great floods in a changing climate. *Nature* 415(6871):514–517
- Milly PCD, Dunne KA, Vecchia AV (2005) Global pattern of trends in streamflow and water availability in a changing climate. *Nature* 438:347–350
- Moraes JM, Pellegrino GQ, Ballester MV, Martinelli LA, Victoria RL, Krusche AV (1998) Trends in hydrological parameters of a southern Brazilian watershed and its relation to human induced changes. *Water Res Manag* 12(4):295–311
- Nathan R, McMahon TA (1990) Evaluation of automated techniques for base flow and recession analyses. *Water Resour Res* 26(7):1465–1473
- Nie CJ, Li HR, Yang LS, Wu SH, Liu Y, Liao YF (2012) Spatial and temporal changes in flooding and the affecting factors in China. *Nat Hazards* 61:425–439

- Piao S, Ciais P, Huang Y, Shen Z, Peng S, Li J, Fang J (2010) The impacts of climate change on water resources and agriculture in China. *Nature* 467(7311):43–51
- Sen Z (1998) Average areal precipitation by percentage weighted polygon method. *J Hydrol Eng* 3(1):69–72
- Sun W, Mu X, Song X, Wu D, Cheng A, Qiu B (2016) Changes in extreme temperature and precipitation events in the loess plateau (china) during 1960–2013 under global warming. *Atmos Res* 168(1):33–48
- UNDP (2004) A global report: reducing disaster risk-a challenge for development. John S. Swift Co., New York
- Villarini G, Smith JA, Serinaldi F, Ntelekos AA, Schwarz U (2012) Analyses of extreme flooding in austria over the period 1951–2006. *Int J Climatol* 32(8):1178–1192
- Wan S, Zhang J, Wang G, Zhang L, Lei C, Amgad E et al (2020) Evaluation of changes in streamflow and the underlying causes: a perspective of an upstream catchment in haihe river basin, china. *J Water Clim Change* 11(1):241–257
- Wang Y, Ding Y, Ye B, Liu F, Wang J (2013) Contributions of climate and human activities to changes in runoff of the Yellow and Yangtze rivers from 1950 to 2008. *Sci China-Earth Sci* 56(8):1398–1412
- Wang F, Hessel R, Mu X, Maroulis J, Zhao G, Geissen V et al (2015) Distinguishing the impacts of human activities and climate variability on runoff and sediment load change based on paired periods with similar weather conditions: a case in the yan river, china. *J Hydrol* 527:884–893
- Wang S, Fu B, Piao S, Lu Y, Ciais P, Feng X, Wang Y (2016a) Reduced sediment transport in the Yellow River due to anthropogenic changes. *Nat Geosci* 9(1):38–41
- Wang G, Zhang J, Yang Q (2016b) Attribution of runoff change for the xinshui river catchment on the loess plateau of china in a changing environment. *Water* 8(6):267
- Wu ZY, Lu GH, Liu ZY, Wang JX, Xiao H (2013) Trends of extreme flood events in the pearl river basin during 1951–2010. *Adv Clim Change Res* 4(2):110–116
- Xu Z, Bennett MT, Tao R, Xu J (2004) China's sloping land conversion programme four years on: current situation, pending issues. *Int for Rev* 6(3):317–326
- Yang Q, Zhang H, Peng W, Lan Y, Luo S, Shao J et al (2019) Assessing climate impact on forest cover in areas undergoing substantial land cover change using landsat imagery. *Sci Total Environ* 659:732–745
- Yuan XP, Lei TW (2004) Soil and water conservation measures and the benefits in runoff and sediment reductions. *Trans CSAE* 20(2):296–300 (in Chinese)
- Zhang Q, Sun P, Chen X, Jiang T (2011) Hydrological extremes in the Poyang Lake basin, China: changing properties, causes and impacts. *Hydrol Process* 25(20):3121–3130
- Zhao G, Tian P, Mu X, Jiao J, Wang F, Gao P (2014b) Quantifying the impact of climate variability and human activities on streamflow in the middle reaches of the yellow river basin, china. *J Hydrol* 519:387–398
- Zhao YZ, Mu XM, Yan BW, Zhao GJ (2014a) Influence of vegetation restoration on runoff and sediment of Yanhe basin. *J Sed Res* 000(004):67–73 (In Chinese)
- Zhiyong W, Guihua L, Zhiyu L, Jinxing W (2012) Trends of extreme flood events in the pearl river basin under climate change. *Progressus Inquisitiones De Mutatione Climatis* 8(6):403–408
- Zhou JQ (2015) Reflection and countermeasure to rainstorm happened on July 3. 2013 in Yanan Area of Shaanxi Province. *China Flood Drought Manag* 3:93–94 (In Chinese)

**Publisher's Note** Springer Nature remains neutral with regard to jurisdictional claims in published maps and institutional affiliations.

## Authors and Affiliations

ChaoJun Gu<sup>1,2</sup> · Yongqing Zhu<sup>1</sup> · Renhua Li<sup>1</sup> · He Yao<sup>1</sup> · Xingmin Mu<sup>2,3</sup>

<sup>1</sup> Yangtze River Basin Monitoring Center Station for Soil and Water Conservation, Changjiang Water Resources Commission, Wuhan 430012, Hubei Province, China

<sup>2</sup> State Key Laboratory of Soil Erosion and Dryland Farming On the Loess Plateau, Northwest A&F University, Xinong Road 26, Yangling 712100, Shaanxi Province, China

<sup>3</sup> Institute of Soil and Water Conservation of Chinese Academy of Sciences and Ministry of Water Resources, Yangling 712100, Shaanxi Province, China